Contrasting transition complexity between El Niño and La Niña: Observations and CMIP5/6 models

Shih-Wei Fang and Jin-Yi Yu*

Department of Earth System Science, University of California, Irvine, CA, USA

Revised, June 2020

Submit to *Geophysical Research Letters*

Key points:

- El Niño transitions are dominated by, in order, episodic, cyclic, and multi-year patterns, but the reversed order is found for La Niña.
- This asymmetry is caused by a subtropical Pacific mechanism that produces more episodic (multi-year) transitions for El Niño (La Niña).
- CMIP5 models fail to simulate the asymmetry due to a cold bias in their tropical mean states and an overly weak subtropical mechanism.

*Corresponding Author: Dr. Jin-Yi Yu, Department of Earth System Science, University of California, Irvine, CA, USA. Email: jyyu@uci.edu

Abstract

The observed El Niño and La Niña exhibit different complexities in their event-to-event transition patterns. The El Niño is dominated in order by episodic, cyclic, and multi-year transitions, but the reversed order is found in the La Niña. A subtropical Pacific onset mechanism is used to explain this difference. This mechanism triggers El Niño/La Niña events via subtropical processes and is responsible for producing multi-year and episodic transitions. Its nonlinear responses to the tropical Pacific mean state result in more multi-year transitions for La Niña than El Niño and more episodic transitions for El Niño than La Niña. The CMIP5/6 models realistically simulate the observed transition complexity of El Niño but fail to simulate the transition complexity of La Niña. This deficiency in CMIP5 models arises from a weaker than observed subtropical onset mechanism and a cold bias in the tropical Pacific mean sea surface temperatures in the models.

Plain Language Summary

A new asymmetry is found between the warm (i.e., El Niño) and cold (i.e., La Niña) phases of El Niño-Southern Oscillation (ENSO) in their event-to-event transition patterns. The observed El Niño transitions is dominated in order by the episodic, cyclic, and multi-year patterns, but the reversed order is found in the La Niña transitions. This difference in the transitions arises from a subtropical Pacific forcing mechanism that triggers ENSO events. The subtropical onset mechanism is found to generate more episodic transitions for El Niño than La Niña and more multi-year transitions for La Niña than El Niño. This asymmetry is due to nonlinear responses of the subtropical mechanism to the tropical mean sea surface temperatures (SSTs). State-of-art global climate models realistically simulate the observed transition complexity of El Niño but fail to reproduce the transition complexity of La Niña. This deficiency arises from a weak subtropical onset mechanism and a cold bias in the tropical Pacific mean SSTs in the models.

1. Introduction

El Niño-Southern Oscillation (ENSO) is a complex phenomenon that involves wide ranges of different patterns, amplitudes and temporal evolutions (Kao and Yu 2009; Capotondi et al. 2015; Wang et al. 2017; Yu et al. 2017; Timmermann et al. 2018; Yu & Fang 2018). One important part of the complexity appears in the way that one ENSO event transitions to another. An El Niño (La Niña) event can be preceded by a La Niña (El Niño) event to result in a cyclic transition, by another El Niño (La Niña) event to become a multi-year transition, or by a neutral (non-ENSO) condition to become an episodic transition (Yu & Fang 2018). ENSO onset mechanisms control how anomalies in sea surface temperature (SST) are established in the equatorial Pacific and play critical roles in controlling transition patterns (Yu & Fang 2018; Wang et al. 2019).

Two primary onset mechanisms of ENSO have been identified: a tropical Pacific onset (TP-onset) mechanism and a subtropical Pacific onset (SP-onset) mechanism (Wang et al. 2017; Yu et al. 2017; Yu & Fang 2018). The TP-onset mechanism invokes equatorial thermocline variations to initiate the sea surface temperature (SST) anomalies associated with ENSO, such as those described by the recharged oscillator (Wyrtki 1975; Jin 1997) and delayed oscillator theories (Battisti & Hirst 1989; Suarez & Schopf 1988; Zebiak & Cane 1987). This mechanism typically produces ENSO SST anomalies first in the eastern equatorial Pacifi, where the thermocline is the shallowest and SSTs are most sensitive to thermocline variations. Yu & Fang (2018) find that the TP-onset mechanism generates mostly the cyclic transition and contributes to reduce ENSO transition complexity, although some complexity may arise from its asymmetric responses to El Niño and La Niña (Hu et al. 2017).

On the other hand, the SP-onset mechanism invokes subtropical Pacific processes to trigger ENSO events (Yu et al. 2010; Yu & Kim 2011). The subtropical processes include those described by the seasonal footprinting mechanism (Vimont et al. 2003; Kao & Yu 2009; Alexander et al. 2010), trade wind charging (Anderson et al. 2013; Anderson & Perez 2015), wind-evaporation-SST feedback (Xie & Philander 1994) and Pacific meridional mode (PMM; Chiang & Vimont 2004). This mechanism typically results in ENSO SST anomalies that first appear in the central equatorial Pacific, where the northeastern Pacific trade winds approach the equator (Yu et al. 2010). Yu & Fang (2018) find that the SP-onset mechanism can result in all three transition patterns and is a key source of ENSO transition complexity.

Recent studies (Yu & Fang 2018; Fang & Yu 2020) reveal that the SP-onset mechanism can be activated by both the warm (i.e, El Niño) and cold (i.e., La Niña) phases of the ENSO. However, the way that the SP-onset mechanism responds to the El Niño is not symmetric to its response to the La Niña. For example, it is relatively easy for a La Niña event to activate the negative phase of SP-onset mechanism and result in another La Niña, but it is not easy for an El Niño event to activate the positive phase of SP-onset mechanism and result in another El Niño. Therefore, it is possible that transition complexity can be different between these two ENSO phases. The goals of this study are to compare the transition complexity between El Niño and La Niña in the observations, and to examine whether the CMIP5/6 models can reproduce the observed complexities, and, if not, to identify model deficiencies and their causes.

2. Datasets and methods

Monthly mean values of SST, surface wind, and sea surface heights (SSH) were regridded to a common grid of 1.5°-longitude by 1°-latitude for analysis. The anomalies were defined as the deviations from the seasonal cycles (calculated from the analysis period 1948-2016) with their linear trends removed. The SST, surface wind, and SSH data are downloaded respectively from the Hadley Center Sea Ice and Sea Surface Temperature data set (HadISST) (Rayner et al. 2003), the National Centers for Environmental Prediction–National Center for Atmospheric Research (NCEP–NCAR) reanalysis (Kalnay et al. 1996), and the German contribution of the Estimating the Circulation and Climate of the Ocean project (□ □ □2015). The same procedures were applied to the last one hundred years of the pre-industrial simulations produced by 34 CMIP5 models (Taylor et al. 2012; see Table S1 for the details of the models) and 20 CMIP6 models (see Table S2). A TP-onset index and a SP-onset index were constructed from the combined SST, surface wind, and SSH anomalies using a multivariate empirical orthogonal function analysis (Xue et al. 2000; Yu & Fang 2018; see Text S1 for details).

Using only the SST information, we identify the transition pattern (i.e., cyclic, multi-year, or episodic) for every El Niño and La Niña event based on the ENSO condition during the previous year (Fig. S1; see Text S2 for detailed descriptions). For example, if an El Niño event is preceded by a La Niña condition during its previous year, we consider that El Niño event to be a cyclic transition event. Table 1 lists the transition pattern and onset calendar month of all El Niño and La Niña events during the analysis period. The same classification methodology is also applied to the CMIP5/6 model simulations.

3. Results

Figure 1a shows that, during the analysis period of 1948-2016, El Niño events are dominated by episodic transitions (52.9%; 9 events), followed by cyclic transitions (35.3%; 6 events), and the least by multi-year transitions (11.8%; 2 events). However, La Niña events have a distinct dominance, where the percentages of multi-year (42.1%; 8 events) and cyclic (42.1%; 8 events) transitions are the most, and episodic transitions become the least (15.8%; 3 events). The El Niño has the most percentage for episodic transitions and the least for multi-year transitions; whereas, the La Niña has, reversely, the most percentage for multi-year transitions and the least for episodic transitions. The transition complexity is thus asymmetric between the El Niño and La Niña phases of the ENSO. The asymmetry comes from the very distinct dominances of the episodic and multi-year transitions, while the cyclic transition accounts for similar percentages in El Niño and La Niña.

To understand the cause of the asymmetry, we contrast the evolutions of equatorial (5°S-5°N) SST anomalies composited for the three transition patterns of El Niño and La Niña (Figs. 2a-f). As expected, ENSO SST anomalies in the cyclic, episodic, and multi-year transitions were preceded by opposite-signed, near-neutral, and same-signed anomalies in the previous year, respectively. It is important to note that the onset locations (during months -3 to 0) of the ENSO SST anomalies are different. The anomalies first appear in the eastern equatorial Pacific for both the cyclic El Niño and La Niña and in the central equatorial Pacific for both the multi-year El Niño and La Niña; whereas the SST anomalies show up in the central equatorial Pacific for the episodic El Niño but in the eastern equatorial Pacific for the episodic La Niña.

As mentioned, the TP-onset mechanism triggers ENSO events in which anomalies appear first in the eastern equatorial Pacific; whereas the SP-onset mechanism triggers ENSO events in which anomalies appear first in the central equatorial Pacific. The locations of SST anomalies in Figs. 2a-f suggest that the onset mechanisms are the same for the cyclic transition (the TP-onset mechanism) and multi-year transition (the SP-onset mechanism) of El Niño and La Niña, but are different for the episodic El Niño and La Niña. While the SP-onset mechanism is more associated with the episodic El Niño, the TP-onset mechanism is more associated with the episodic La Niña. The values of the TP-onset and SP-onset indices during the onset period of each transition (see months -3 to month 0 in Figs. S1a-f) confirm this. Therefore, the causes of the asymmetric transition complexity are related to how these different mechanisms result in more frequent episodic El Niños than episodic La Niñas and how the SP-onset mechanism results in more multi-year La Niñas than El Niños.

Figure 2e shows that the episodic La Niña is preceded by weak warming. This evolution pattern is similar to that of the cyclic La Niña, except that in the episodic La Niña the warming is not strong enough to be classified as an El Niño. Their associated thermocline evolutions (represented by the SSH anomalies; Figs. S4d and e) are both characterized by a graduate shallowing of the thermocline depth during the preceding year. This indicates that the weak SST warming in the previous year discharges the equatorial Pacific to onset the La Niña. This confirms the contribution of the TP-onset mechanism to the episodic La Niña. On the other hand, one-third of episodic El Niño events are also more associated with the TP-onset mechanism (Fig. S5e-f), even though the majority of episodic El Niños are associated with the SP-onset mechanism. These results indicate that the TP-onset mechanism can generate both episodic El Niños and La Niñas, but the episodic El Niño can also be additionally produced by the SP-onset mechanism. The fact that the SP-onset mechanism favors to produce episodic El Niños but not La Niñas can explain why episodic events account for a larger percentage of El Niños (52.9%) than La Niñas (15.8%).

Previous studies have shown that the SP-onset mechanism is more capable of producing episodic El Niño events than episodic La Niña events (e.g., Larson & Kirtman 2013). One explanation for this is that an anomalous warming in the central equatorial Pacific can excite a stronger atmospheric feedback and more westerly winds than an anomalous cooling that induces easterly winds in the same region (Chen & Majda 2016; Chen et al. 2019). Therefore, the initial warming triggered by the SP-onset mechanism in the central equatorial Pacific has a larger chance to develop into an episodic El Niño, but the initial equatorial cooling triggered by the SP-onset mechanism has a smaller chance to develop into an episodic La Niña.

As for the reason why the SP-onset mechanism produces more multi-year La Niñas than multi-year El Niños, Fang & Yu (2020) have offered an explanation. They find the occurrence frequencies of the multi-year El Niño and La Niña are controlled by the mean SSTs in the central equatorial Pacific. With a mean SST there that is slightly higher than the threshold temperature (28°C) for deep convection, a La Niña cooling in the region can abruptly turn off the deep convection. This generates a strong heating anomaly that excites a stronger wavetrain response than a comparable El Niño warming in this region (Lyu et al. 2017; Stuecker 2018; Fang & Yu 2020). The stronger (weaker) wavetrain response is more (less) capable of activating the SP-onset mechanism and to onset another La Niña (El Niño) in the following year. Therefore, present-day mean SSTs in the equatorial Pacific favor more multi-year La Niña transitions than multi-year El Niño transitions.

We next examine whether CMIP5 models can simulate the differences in transition frequencies between El Niño and La Niña described above. Pre-industrial simulations produced by thirty-four CMIP5 models were analyzed (Table S1). Their multi-model means (MMM) (Fig. 1b) show that the simulated El Niño has a similar transition complexity as in the observations. Episodic El Niño transitions account for the highest percentage (49.93%), followed by cyclic El Niño transition (32.27%), with multi-year El Niño transitions least frequent (17.80%). However, the CMIP5 models cannot reproduce the observed frequency of occurrence of the La Niña transition patterns. While the multi-year La Niña transition accounts for the highest observed percentage, it accounts for the least of the simulated La Niña transitions (22.3%). The leading transition pattern for the simulated La Niña is the cyclic transition (43.18%) followed by the episodic transition (34.5%).

We further examine the transition complexity in each individual CMIP5 model and present the results using an ENSO Transition Complexity (ETC) diagram

(Fig. 3). In the diagram, the x- and y-axis values are, respectively, the percentages of episodic and multi-year transitions in each model. The percentage of cyclic transitions, which can be calculated as “100 - (x-axis value + y-axis values)”, is represented by the circle size (larger dots for higher percentages). Based on all possible values on the x-axis and y-axis, we can divide the ETC diagram into regions where cyclic, episodic, or multi-year transition has the largest percentage and dominates the transitions. Figure 3a shows that all but two CMIP5 models realistically produce more episodic El Niños than multi-year El Niños (i.e., below the dashed line of x=y), and that all but seven models have El Niño transitions that are dominated by the episodic type. The observed transition complexity of El Niños is realistically reproduced in most of the CMIP5 models.

The ETC diagram for La Niña (Fig. 3b) reveals which transitions are responsible for the model deficiency. Only five CMIP5 models produce more multi-year La Niñas than episodic La Niñas (i.e., above the dashed line of x=y), and no model has La Niña transitions that are dominated by multi-year transitions. The CMIP5 models have a tendency to simulate too many episodic La Niñas and too few multi-year La Niñas, failing to reproduce the observed transition complexity of La Niña.

To identify the sources of these model deficiencies, we examine the MMM evolutions of the equatorial SST anomalies during the three transitions (Figs. 2g-l). Overall, all three transitions for the simulated El Niño and La Niña have onset locations similar to those in the observations. This similarity implies that the underlying transition dynamics in the models are similar to those in the observations.

The relative strengths of the TP-onset and the SP-onset indices in the models also confirm this assertion (Fig. S2). The SP-onset index is relatively stronger than the TP-onset index in the episodic El Niño, multi-year El Niño, and multi-year La Niña. In contrast, the TP-onset index is relatively stronger than the SP-onset index in the episodic La Niña, cyclic El Niño, and cyclic La Niña. However, we notice that the episodic El Niños in the models also show an onset signature in the eastern equatorial Pacific which is absent in the observations. This difference suggests that the models have an overly strong TP-onset mechanism. We find that in about half of the CMIP5 models (16/34) the episodic El Niño is more associated with the TP-onset mechanism (Fig. S6e-f). This is consistent with Yu & Fang (2018) who find most CMIP5 models have stronger than observed TP-onset mechanisms and weaker than observed SP-onset mechanisms. Since the episodic El Niño can be generated by both mechanisms, the frequency of occurrence of the episodic El Niño in the models may not be much different from observations in spite of the weaknesses noted in the simulations of the two onset mechanisms. In contrast, the episodic La Niña is produced primarily by the TP-onset mechanism, leading to an overestimation of episodic La Niña events in the models (34.5% vs 15.8% in the observations).

The recent study of Fang and Yu (2020) has suggested that the slightly above 28°C mean SST in the central equatorial Pacific is a reason why the SP-onset mechanism produces more multi-year La Niñas than multi-year El Niños in the observations. Our finding that the CMIP5 models produce a smaller asymmetry between the numbers of multi-year El Niños and La Niñas (22.3% vs. 17.8%; see Fig. 1b) implies that the mean SSTs in the models are different from the observations. To examine this possibility, we contrast in Figure 4 the mean SSTs in the tropical Pacific between the five models that produce the most multi-year La Niñas and the five models that produce most multi-year El Niños (see Fig. S7 for the models). The group with more multi-year La Niñas (Fig. 4b) has mean SSTs that are similar to the observations (Fig. 4a), slightly warmer than the 28°C in the central equatorial Pacific (red boxes in Fig. 4). In contrast, the group with more multi-year El Niños (Fig. 4c) shows much colder mean SSTs in the central equatorial Pacific (27.3°C). This is consistent with the suggestion of Fang & Yu (2020) that a warmer (colder) mean SST in the equatorial central Pacific favors more multi-year La Niña (El Niño) events.

Contemporary models are known to have a tendency to produce a lower than observed mean SSTs in the central equatorial Pacific associated with a cold tongue that extends further westward than observed (Davey et al. 2001; Misra et al. 2008; Vannière et al. 2012; Li et al. 2016). We therefore examine in Figure 4d the relationship between the model differences in multi-year transitions and the model mean SSTs across the equatorial Pacific (5°S-5°N and 140°E-120°W; black boxes in Fig. 4). A significant (at 99% level) linear relationship exists between these two quantities. The colder the mean equatorial SSTs in the model, the stronger tendency to have more multi-year El Niños. The MMM value of the mean SST (26.5 °C) is colder than the observed value (27.3 °C), leading to the weaker tendency for more multi-year La Niñas in the models. The well-known cold bias in the equatorial Pacific is a key reason why the CMIP5 models cannot reproduce the observed El Niño-La Niña asymmetry in multi-year transitions.

We repeated the analyses with 20 CMIP6 models (Figs. S3) and obtained similar results (Fig. 1c). The CMIP6 models does not show any significant improvement over CMIP5 models in the simulation of ENSO transition complexity. Similar to the CMIP5 models, the CMIP6 models also reproduce the observed transitions for El Niño but fail to reproduce the La Niña transitions (Fig. 1c and S8). The three transition patterns and their associated onset mechanisms are also similar to the CMIP5 models (Fig. S9). The TP-onset mechanism is overestimated in the CMIP6 models, while the SP-onset mechanism is underestimated (Fig. S10). A similar but weaker relation exists between the cold tongue bias and the multi-year La Niña tendency in the CMIP6 models (Fig. S11 and S12). This weaker tendency reveals that differences exist in the simulated ENSO transition complexity between the CMIP5 and CMIP6 models (e.g. distinct atmospheric responses in CMIP models), even though both sets of models fail to reproduce the observed transition complexity for La Niña.

4. Summary and Discussion

In this study, we find that there are more episodic El Niños than La Niñas and more multi-year La Niñas than El Niños in the observations. This difference is the result of the nonlinear characteristics of the SP-onset mechanism. Our findings further confirm the critical roles of the SP-onset mechanism in determining the ENSO transition complexity and the transition asymmetry between the El Niño and La Niña. We find that the CMIP5 and CMIP6 models can reproduce the transition complexity for El Niño but not for La Niña. The models tend to produce too many episodic La

Niña events and too few multi-year La Niña events. We are able to link the former deficiency to a weaker than observed SP-onset mechanism in the CMIP5/6 models and the latter to a cold bias in mean state SSTs in the equatorial Pacific in the CMIP5 models. To achieve better simulations of ENSO transition complexity, further efforts are to improve the model deficiencies in simulating the SP-onset mechanism and mean SSTs in the equatorial Pacific.

***Acknowledgments*:**

We thank two anonymous reviewers for their valuable comments. This research is supported by NSF's Climate & Large-scale Dynamics Program under Grants AGS-1833075. The HadISST SST data were downloaded from their site (http://www.metoffice.gov.uk/hadobs/hadisst/data/download.html). The wind fields of NCEP/NCAR were obtained from NOAA (https://www.esrl.noaa.gov/psd/). The GECCO2 SSH data sets were downloaded from the Integrated Climate Data Center (https://icdc.cen.uni-hamburg.de/en/gecco2.html). We acknowledge the World Climate Research Programme's Working Group on Coupled Modelling, which is responsible for CMIP, and we thank the climate modeling groups (listed in Table S1 and S2 of this paper) for producing and making available their model output. For CMIP the U.S. Department of Energy's Program for Climate Model Diagnosis and Intercomparison provides coordinating support and led the development of the software infrastructure in partnership with the Global Organization for Earth System Science Portals.

References

Alexander, M. A., Vimont, D. J., Chang, P., & Scott, J. D. (2010). The impact of extratropical atmospheric variability on ENSO: Testing the seasonal footprinting mechanism using coupled model experiments. *Journal of Climate*, *23*(11), 2885-2901.

Anderson, B. T., Perez, R.C. & Karspeck, A.. (2013). Triggering of El Niño onset through trade wind–induced charging of the equatorial Pacific. *Geophysical Research Letters,* 40.6, 1212-1216.

Anderson, B. T., & Perez, R. C. (2015). ENSO and non-ENSO induced charging and discharging of the equatorial Pacific. *Climate Dynamics*, *45*(9-10), 2309-2327.

Battisti, D. S. & Anthony C. H. (1989) Interannual variability in a tropical atmosphere–ocean model: Influence of the basic state, ocean geometry and nonlinearity. *Journal of the atmospheric sciences,* 46.12, 1687-1712.

Capotondi, A., Wittenberg, A. T., Newman, M., Di Lorenzo, E., Yu, J. Y., Braconnot, P., ... & Jin, F. F. (2015). Understanding ENSO diversity. *Bulletin of the American Meteorological Society*, *96*(6), 921-938.

Chen, N., & Majda, A. J. (2016). Simple dynamical models capturing the key features of the Central Pacific El Niño. *Proceedings of the National Academy of Sciences*, *113*(42), 11732-11737.

Chen, N., Thual, S., & Stuecker, M. F. (2019). El Niño and the Southern Oscillation: Theory. Book Chapter in *Reference Module in Earth Systems and Environmental Sciences.*

Chiang, J. C., & Vimont, D. J. (2004). Analogous Pacific and Atlantic meridional modes of tropical atmosphere–ocean variability. *Journal of Climate*, *17*(21), 4143-4158.

Davey, M. et al. (2002) STOIC: a study of coupled model climatology and variability in tropical ocean regions. *Climate Dynamics,* 18.5, 403-420.

Fang, S.-W., & Yu, J.-Y. (2020). A Control of ENSO Transition Complexity by Tropical Pacific Mean SSTs through Tropical-Subtropical Interaction. *Geophysical Research Letters*, 47, e2020GL087933. https://doi.org/10.1029/2020GL087933

Jin, F. F. 1997. An equatorial ocean recharge paradigm for ENSO. Part I: Conceptual model. *Journal of the Atmospheric Sciences*, *54*(7), 811-829.

Hu, Z. Z., Kumar, A., Huang, B., Zhu, J., Zhang, R. H., & Jin, F. F. (2017). Asymmetric evolution of El Niño and La Niña: the recharge/discharge processes and role of the off-equatorial sea surface height anomaly. *Climate Dynamics*, *49*(7-8), 2737-2748.

Kalnay, E., Kanamitsu, M., Kistler, R., Collins, W., Deaven, D., Gandin, L., ... & Zhu, Y. (1996). The NCEP/NCAR 40-year reanalysis project. *Bulletin of the American meteorological Society*, *77*(3), 437-471.

Kao, H. Y., & Yu, J. Y. (2009). Contrasting eastern-Pacific and central-Pacific types of ENSO. *Journal of Climate*, *22*(3), 615-632.

Köhl, A. (2015). Evaluation of the GECCO2 ocean synthesis: transports of volume, heat and freshwater in the Atlantic. *Quarterly Journal of the Royal Meteorological Society*, *141*(686), 166-181.

Larson, S., & Kirtman, B. (2013). The Pacific Meridional Mode as a trigger for ENSO in a high-resolution coupled model. *Geophysical Research Letters*, *40*(12), 3189-3194.

Li, G., Xie, S. P., Du, Y., & Luo, Y. (2016). Effects of excessive equatorial cold tongue bias on the projections of tropical Pacific climate change. Part I: The warming pattern in CMIP5 multi-model ensemble. *Climate dynamics*, *47*(12), 3817-3831.

Lyu, K., Yu, J. Y., & Paek, H. (2017). The influences of the Atlantic multidecadal oscillation on the mean strength of the North Pacific subtropical high during boreal winter. *Journal of Climate*, *30*(1), 411-426.

Misra, V., Marx, L., Brunke, M., & Zeng, X. (2008). The equatorial Pacific cold tongue bias in a coupled climate model. *Journal of climate*, *21*(22), 5852-5869.

Rayner, N. A., Parker, D. E., Horton, E. B., Folland, C. K., Alexander, L. V., Rowell, D. P., ... & Kaplan, A. (2003). Global analyses of sea surface temperature, sea ice, and night marine air temperature since the late nineteenth century. *Journal of Geophysical Research: Atmospheres*, *108*(D14).

Stuecker, M. F. (2018). Revisiting the Pacific meridional mode. *Scientific reports*, *8*(1), 1-9.

Suarez, M. J., & Schopf, P. S. (1988). A delayed action oscillator for ENSO. *Journal of the atmospheric Sciences*, *45*(21), 3283-3287.

Taylor, K. E., Stouffer, R. J., & Meehl, G. A. (2012). An overview of CMIP5 and the experiment design. *Bulletin of the American Meteorological Society*, *93*(4), 485-498.

Timmermann, A., An, S. I., Kug, J. S., Jin, F. F., Cai, W., Capotondi, A., ... & Stein, K. (2018). El Niño–southern oscillation complexity. *Nature*, *559*(7715), 535-545.

Vannière, B., Guilyardi, E., Madec, G., Doblas-Reyes, F. J., & Woolnough, S. (2013). Using seasonal hindcasts to understand the origin of the equatorial cold tongue bias in CGCMs and its impact on ENSO. *Climate dynamics*, *40*(3-4), 963-981.

Vimont, D. J., Wallace, J. M., & Battisti, D. S. (2003). The seasonal footprinting mechanism in the Pacific: Implications for ENSO. *Journal of Climate*, *16*(16), 2668-2675.

Wang, C., Deser, C., Yu, J. Y., DiNezio, P., & Clement, A. (2017). El Niño and Southern Oscillation (ENSO): A Review. In *Coral Reefs of the Eastern Tropical Pacific* (pp. 85-106). Springer Netherlands.

Wang, B. et al. (2019). Historical change of El Niño properties sheds light on future changes of extreme El Niño.. *Proceedings of the National Academy of Sciences,* 116.45, 22512-22517.

Wyrtki, K. (1975). El Niño—the dynamic response of the equatorial Pacific Oceanto atmospheric forcing. *Journal of Physical Oceanography*, *5*(4), 572-584.

Xie, S. P., & Philander, S. G. H. (1994). A coupled ocean-atmosphere model of relevance to the ITCZ in the eastern Pacific. *Tellus A*, *46*(4), 340-350.

Xue, Y., Leetmaa, A., & Ji, M. (2000). ENSO prediction with Markov models: The impact of sea level. *Journal of Climate*, *13*(4), 849-871.

Yu, J-Y, & Fang S-W. (2018). The Distinct Contributions of the Seasonal Footprinting and Charged-Discharged Mechanisms to ENSO Complexity. *Geophysical Research Letters,* 45.13, 6611-6618.

Yu, J. Y., Kao, H. Y., & Lee, T. (2010). Subtropics-related interannual sea surface temperature variability in the central equatorial Pacific. *Journal of Climate*, *23*(11), 2869-2884.

Yu, J.-Y., X. Wang, S. Yang, H. Paek, and M. Chen (2017). Changing El Niño-Southern Oscillation and Associated Climate Extremes, Book Chapter in *Climate Extremes: Patterns and Mechanisms*, Wang, S.-Y., Jin-Ho Yoon, Chris Funk, and R. R. Gillies (Ed.), AGU Geophysical Monograph Series, Vol. 226, Pages 3-38.

Zebiak, S. E., & Cane, M. A. (1987). A model El Niño–southern oscillation. *Monthly Weather Review*, *115*(10), 2262-2278.

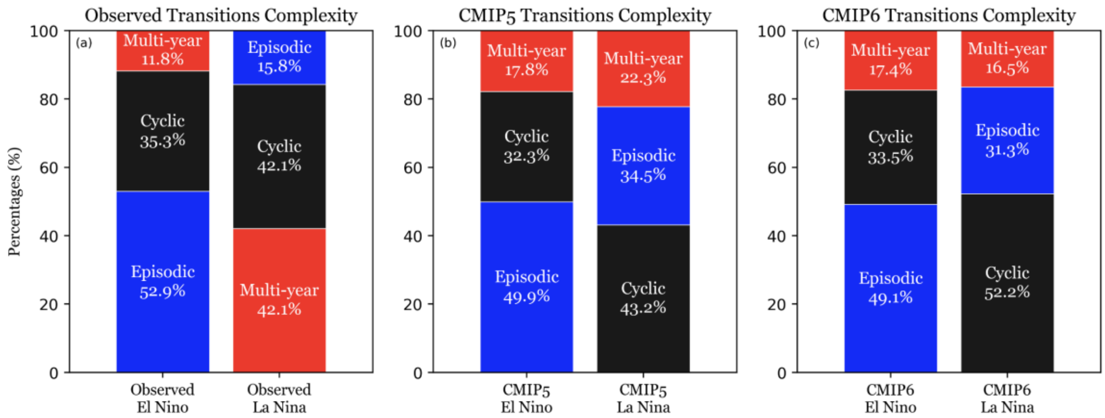

Figure 1. The transition complexity of El Niño (left bars) and La Niña (right bars) in (a) the observations, (b) the multi-model mean from thirty-four CMIP5 models, and (c) the multi-model mean from twenty CMIP6 models. The percentages of the transitions are ordered from highest (bottom) to lowest (top).

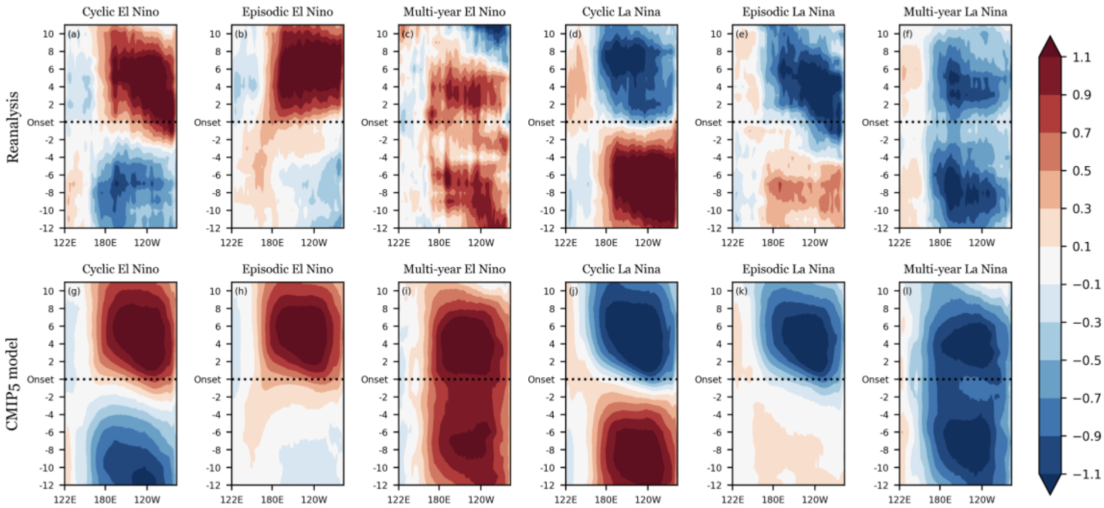

Figure 2. Evolutions of equatorial (5°S-5°N) Pacific SST anomalies composited for the cyclic, episodic, and multi-year transitions of (a)-(c) El Niño and (d)-(f) La Niña in the reanalysis and (g)-(i) for the simulated El Niños and (j)-(l) La Niñas in the multi-model mean of CMIP5 simulations. The events are composited based on their onset time. Shadings are SST anomalies from 12 months before the ENSO onset month to 12 months after.

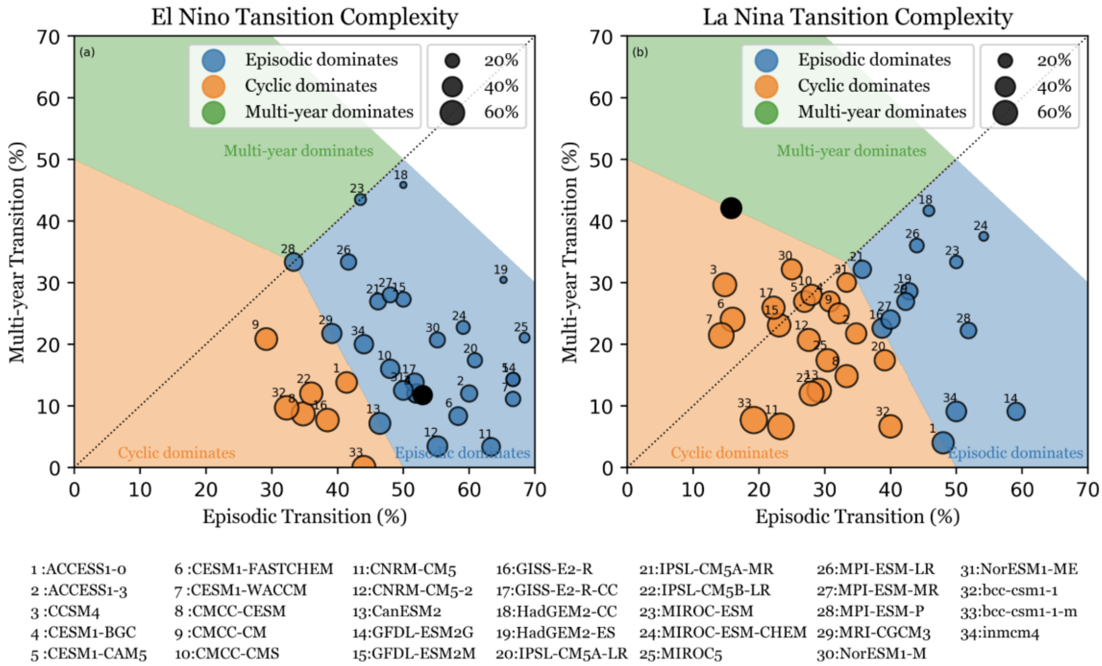

Figure 3. ENSO transition complexity (ETC) diagrams for (a) the simulated El Niño and (b) the La Niña in CMIP5 models in CMIP5 models. The x-axis and y-axis are, respectively, the percentage of episodic transitions and multi-year transitions in each model. The size of the circles is proportional to the percentage of cyclic transitions. The color of the circle indicates the highest percentage of transitions: orange for cyclic, blue for episodic, and green for multi-year transition. The same color scheme is used in the background shadings to indicate the regions of the diagram where each of the three transitions is most frequent. The black dot is the observations and the CMIP5 models are labeled with their corresponding numbers.

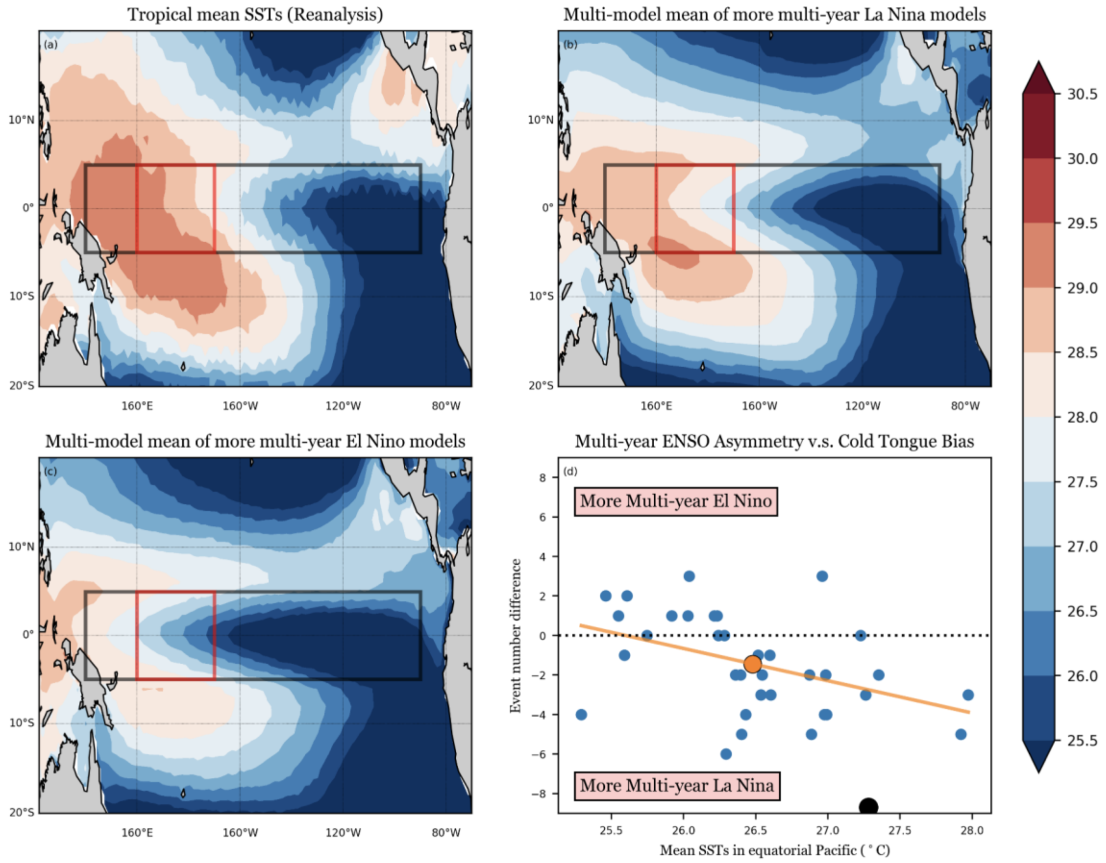

Figure 4. (a) Mean SSTs in the tropical Pacific calculated from (a) the observations during 1948-2016, (b) the five CMIP5 models with the most multi-year El Niños in Fig. S7, and (c) the five CMIP5 models with the most multi-year La Niñas. The red box denotes the equatorial central Pacific region (5°S-5°N and 160°E-170°W). Panel (d) displays the relationship between the event number difference and the mean SST across the equatorial Pacific (5°S-5°N and 140°E-120°W; the black box). The black dot is the reanalysis value (scaled to event numbers in 100 years as in model simulation), and the orange dot is the multi-model mean value with the orange line representing the linear regression (passing 99% significance test).

El Niño	Transition	Onset (Mon)	La Niña	Transition	Onset (Mon)
1951	Cyclic	6	1949	Episodic	9
1957	Cyclic	4	1954	Episodic	5
1963	Episodic	6	1955	Multi-year	2
1965	Cyclic	5	1956	Multi-year	6
1968	Episodic	10	1964	Cyclic	4
1969	Multi-year	8	1970	Cyclic	6
1972	Cyclic	5	1973	Cyclic	5
1976	Cyclic	8	1975	Multi-year	3
1977	Multi-year	8	1983	Cyclic	9
1982	Episodic	4	1984	Multi-year	9
1986	Episodic	8	1988	Cyclic	4
1991	Episodic	9	1995	Cyclic	8
1994	Episodic	8	1998	Cyclic	6
1997	Episodic	4	1999	Multi-year	8
2002	Episodic	6	2000	Multi-year	9
2009	Cyclic	7	2007	Episodic	7
2015	Episodic	3	2008	Multi-year	10
			2010	Cyclic	5
			2011	Multi-year	7

Table 1. Classification of ENSO transitions and their calendar onset months during the analysis period (1948-2016).